A control systems analysis of HIV prevention model using impulsive input

H.J. Chang [a,*], C.H. Moog [b], A. Astolfi [c,d], P.S. Rivadeneira [b,e]

[a] School of Electrical Engineering, Kookmin University, Seoul 136-702, Republic of Korea
[b] IRCCyN, UMR-CNRS 6597, 1 Rue de la Noë, 44321 Nantes Cedex 03, France
[c] Department of Electrical and Electronic Engineering, Imperial College London, London SW7 2AZ, UK
[d] DICII, Università di Roma Tor Vergata, Via del Politecnico 1, 00133 Roma, Italy
[e] "Grupo de Sistemas No Lineales", INTEC-Facultad de Ingeniería Química (UNL-CONICET), Güemes 3450, 3000 Santa Fe, Argentina

ARTICLE INFO

ABSTRACT

We investigate a control systems analysis on HIV infection dynamics with regard to enhancement of the immune response. The HIV dynamic model is modified to include the pharmacokinetics and pharmacodynamics of antiretroviral HIV drugs, and the intake of drug is considered as impulsive control input. As it is administrated at discrete time instants, we assume that this yields an impulsive control problem for a nonlinear continuous-time system. Based on this new model, we study clinical experiments about antirretoviral treatments via numerical simulation and analyse the experimental results. It is noted that this modeling approach can help to provide a theoretical explanation of the clinical results. The analysis result in the paper could imply that the protocol of the experiment might enhance the immune response against HIV.

1. Introduction

Acquired immune deficiency syndrome (AIDS) is caused by the human immunodeficiency virus (HIV). After HIV infection, CD4 T-cells are infected by the virus. An infected CD4 T-cell does not perform its role in the human immune system and makes multiple HIV copies. With a low level of CD4 T-cell count, the human immune system cannot work properly.

HIV/AIDS is still a prevalent and lethal infectious disease worldwide. In 2009 the estimated number of HIV-infected people was 33.3 million and 1.8 million people died of AIDS [1]. Several studies have reported model-based approaches to understand the HIV/AIDS infection process. Some examples of HIV dynamic models are found in [2,3] and control theoretic studies of the authors, based on the HIV models in [3], are reported in [4,5].

In this paper we research a control scheme using a model-based approach to enhance the human immune response in HIV infection dynamics.[1] The control method is applied to the HIV model in [3],

together with the pharmacological dynamics in [7,8], on the basis of the immune boosting process analysed by the authors in [5].

The research in this paper is supported by the experimental data recently published in [9,10]. Although our research can be applicable to analyse the data of [10], we focus on the experimental result of [9]. Note that we do not analyse the properties of the controlled system formally, which will be done elsewhere, but focus on the conceptual method of the controller design, as well as on the application to the HIV infection dynamics.

This paper contains two major contributions. First, it presents a model modification based on an existing HIV model, considering pharmacological dynamics. The modification introduces dynamic equations describing the pharmacokinetics and pharmacodynamics of antiretroviral drugs. In addition we assume that the controlled drug intake can be considered as impulsive control input for the mathematical model, although in general the drugs are taken orally as extended-release formulation (see [11] for more details). Impulsive control gives a sudden change of the state variable at discrete instants (see [12] for rigorous definition of impulsive control). The modified model is able to accurately describe the effect on HIV patients of a drug regimen. This model helps to study HIV infection dynamics with a realistic regimen of HIV therapy.

Second, the experimental results in [9] can be explained by the immune system analysis on the modified HIV model in the paper. The clinical work of [9] leads to the application of a mathematical

* Corresponding author.
E-mail addresses: hchang@kookmin.ac.kr (H.J. Chang),
Claude.Moog@irccyn.ec-nantes.fr (C.H. Moog), a.astolfi@ic.ac.uk (A. Astolfi),
psrivade@santafe-conicet.gov.ar (P.S. Rivadeneira).
[1] A preliminary version of this paper has been published in [6].

approach to the HIV dynamics. Based on the modified HIV model we obtain an insight into the result of [9], providing an interpretation of the experiment. By analysing the simulation study it is implied that the protocol of the experiment might enhance the immune response against HIV.

The paper is organised as follows. The proposed modeling method is presented in Section 2. Particularly Section 2.1 gives a brief description of the experiments in [9]. Then in Section 2.2 we recall some of the analysis of [5] for the HIV dynamic model of [3] and we modify the model to study numerical realisation of the experiments in [9]. Then Section 3 reports the numerical results with the modified HIV infection model. Finally we discuss the results and conclude the paper in Section 4.

2. Methods

2.1. A summary of the experiments in Grant et al. [9]

Antiretroviral chemoprophylaxis prior to exposure to HIV is regarded as a promising approach for the prevention of HIV infection[13,14]. In [13] it has been shown that the side effect of daily preexposure with tenofovir disoproxil fumarate (TDF) is acceptable while in [14] it has been shown that HIV infection rates of women is decreased up to 39% using a tenofovir 1% vaginal gel. For men and transgender women who have sex with men the current use of preexposure prophylaxis is not common, however most of these people are willing to consider such use if evidence of safety and efficacy were provided [15,16].

We now briefly discuss the experiments of [9]. To evaluate the clinical effect of preexposure chemoprophylaxis, experiments have been designed and conducted in [9]. The experiments assigned 2499 HIV-negative subjects randomly to take a combination of two antiretroviral drugs, i.e. emtricitabine and tenofovir disoproxil fumarate (FTC-TDF), or placebo once a day.

The subjects were observed for 3324 person-years (median, 1.2 years; maximum, 2.8 years). For the studied subjects 10 were revealed to have been infected with HIV at enrollment and 100 became infected with HIV during the follow-up, among which 36 and 64 were in the FTC-TDF and the placebo groups, respectively, implying a 44% reduction in the HIV incidence.

Thus the experimental result concludes that oral FTC-TDF could provide protection against the acquisition of HIV infection. For a complete description of the experiment and the data see [9] and the Supplementary Appendix available at NEJM.org.

Following the pioneering work in [9], over the past few years there have been considerable advances in the issues of the suppression of HIV transmission by using antiretroviral drug [17] with new scientific findings including the results in [18–20]. In [18] it has been shown that, compared to the delayed initiation of anti-HIV therapy, the early initiation reduces the rate of HIV transmission in couples. Particularly the protection against HIV infection in heterosexual men and women has been studied in [20] with daily intake of FTC-TDF, while in [19] it has been concluded that both TDF and FTC-TDF can prevent HIV infection in heterosexual subjects.

2.2. Modeling of HIV dynamics with impulsive control input

In this subsection we consider the HIV infection model of [3] and modify this model including the pharmacokinetics and pharmacodynamics of the FTC-TDF as considered in [9].

2.2.1. HIV infection model with CTL response
The model of [3,21] is given by

$$\dot{x} = \lambda - dx - (1 - \eta)\beta xy, \tag{1}$$

Table 1
HIV model parameters and values [3]

Parameters	Value	Parameters	Value
λ	1	d	0.1
β	1	a	0.2
p_1	1	p_2	1
c_1	0.03	c_2	0.06
q	0.5	b_1	0.1
b_2	0.01	h	0.1

$$\dot{y} = (1 - \eta)\beta xy - ay - p_1 z_1 y - p_2 z_2 y, \tag{2}$$

$$\dot{z}_1 = c_1 z_1 y - b_1 z_1, \tag{3}$$

$$\dot{w} = c_2 xyw - c_2 qyw - b_2 w, \tag{4}$$

$$\dot{z}_2 = c_2 qyw - hz_2, \tag{5}$$

where the states are the populations of specific cells in a unit volume of blood. x, y, z_1, w, and z_2 describe the concentrations of uninfected CD4 T-cells, infected CD4 T-cells, helper-independent CTLs, CTL precursors, and helper-dependent CTLs, respectively.

The quantity η varies between 0 and 1 and describes the control input affecting the parameter β. From a control perspective it represents the efficacy of the drug of the anti-retroviral therapy. If $\eta = 1$ a patient receives the maximal effect of drug (i.e. 100% block of HIV infection process), while $\eta = 0$ means no effect. The remaining parameters λ, d, β, a, p_1, p_2, c_1, c_2, q, b_1, b_2, and h are positive constants. For a detailed explanation of the model see [3].

2.2.2. Analysis of the model
Now we show that the Wodarz model ((1)–(5)) displays 5 equilibrium points [3,6], including a HIV-free equilibrium, a LTNP equilibrium, and other which the virus dominates. The basin of attraction of the third equilibrium is estimated. This lower order model of the HIV-dynamics is shown to be maximally nonlinear in the sense that the largest possible linearization by a state feedback has dimension 2. The three important equilibria are given in what follows.

Point A:

$$x^{(A)} = \frac{\lambda}{d}, \quad y^{(A)} = 0, \quad z_1^{(A)} = 0, \quad w^{(A)} = 0, \quad z_2^{(A)} = 0.$$

Point B:

$$x^{(B)} = \frac{\lambda c_1}{dc_1 + b_1(1 - \eta)\beta}, \quad y^{(B)} = \frac{b_1}{c_1}, \quad z_1^{(B)} = \frac{(1 - \eta)\beta x^{(B)} - a}{p_1},$$

$$w^{(B)} = 0, \quad z_2^{(B)} = 0.$$

Point C:

$$y^{(C)} = \frac{\theta(\eta) - \sqrt{\theta(\eta)^2 - 4(1 - \eta)\beta c_2 q db_2}}{2(1 - \eta)\beta c_2 q},$$

$$x^{(C)} = \frac{\lambda}{d + (1 - \eta)\beta y^{(C)}}, \quad z_1^{(C)} = 0, \quad w^{(C)} = \frac{hz_2^{(C)}}{c_2 qy^{(C)}},$$

$$z_2^{(C)} = \frac{y^{(C)}(c_2(1 - \eta)\beta q - c_2 a) + b_2(1 - \eta)\beta}{c_2 p_2 y^{(C)}},$$

where $\theta(\eta) = c_2(\lambda - dq) - b_2(1 - \eta)\beta$.

The values of the model parameters suggested in [3] for the HIV model are summarised in Table 1. Note that these parameters in [3] are normalised, with which the HIV model can show bistability phenomenon.

With this parameter set and $\eta = 0$ (i.e., no drug treatment), Point A, B and C are $x_A = (10, 0, 0, 0, 0)$, $x_B = (0.2913, 3.3333, 0.0913, 0, 0)$, and $x_C = (8.2255, 0.0216, 0, 1240, 8.0255)$, respectively. In [3], the model ((1)–(5)), with the parameter set of Table 1, has been shown to be bistable when the drug treatment is stopped.
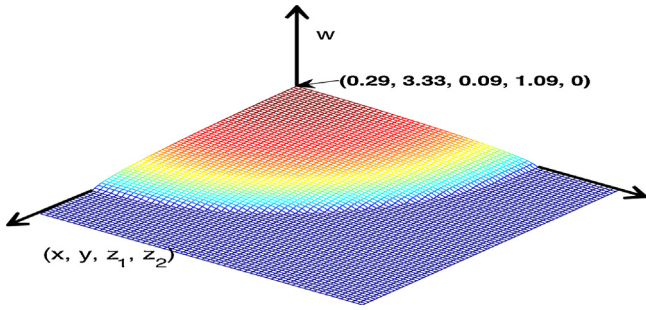
Fig. 1. A qualitative scheme of the basin of attraction of equilibrium B.

The interpretation of each point with the assumption $\eta = 0$ is as follows:

Point A represents the status of a person without HIV. Point A is unstable. It means that the model represents the situation that it is difficult to revert a HIV positive patient back to the HIV-free status if the medication is stopped.

Point C displays the status of a HIV patient not progressing to AIDS, which corresponds to the LTNP status. Because Point C is locally exponentially stable, one control goal is to steer the state near Point C.

Point B corresponds to the status of a HIV patient for whom the virus dominates, and it is stable. Its basin of attraction has the following characteristics: (i) its projection onto the w axis is smaller than its projection onto the (x, y, z_1, z_2)-axis. A trajectory will remain inside the basin of attraction provided the initial value of w is in $[0, 1.09]$ (for the set of parameter of Table 1) whereas for the other variables may be significantly large. In Fig. 1, the basin of attraction is represented qualitatively and displays some narrow size in the w direction. A conclusion of this is if the states x, y, z_1, and z_2 are

in the equilibrium B but somehow w is boosted up to certain level, then the system will leave it.

If we desire to enhance immunity this can be achieved by boosting z_1, w, and z_2. In particular helper-dependent immune responses via w and z_2 should be boosted to lead a patient to the LTNP status (Point C), since the w and z_2 components of Point B are zeros while those of Point C have positive levels. z_2 depends upon w in Eq. (5), which suggests increasing w to drive the patient state towards the LTNP status. Note that Eq. (4) is rewritten as $\dot{w} = K(x, y)w$, where $K(x, y) = c_2xy - c_2qy - b_2$. Now the function $K(x, y)$ depends on the variables x and y. We note that if we force the patient state into the region[2] $K(x, y) > 0$ then the immunity can be enhanced.

Now, we are interested to study the accessibility property of this model. Without loss of generality assume that $u(t) = 1 - \eta(t)$ is the control variable and rewrite the dynamics of the model as:

$$\dot{\zeta}(t) = f(\zeta) + g(\zeta)u(t), \tag{6}$$

$$f = \begin{pmatrix} \lambda - dx \\ -ay - p_1z_1y - p_2z_2y \\ c_1z_1y - b_1z_1 \\ c_2xyw - c_2qyw - b_2w \\ c_2qyw - hz_2 \end{pmatrix}, \quad g = \begin{pmatrix} -\beta xy \\ \beta xy \\ 0 \\ 0 \\ 0 \end{pmatrix}, \tag{7}$$

the sequence $\mathcal{H}_k$ (see [22] for more details) is calculated to characterize the accessibility, that is

$$\mathcal{H}_1 = Span_{\mathcal{K}} \left\{ dx, dy, dz_1, dw, dz_2 \right\},$$

$$\mathcal{H}_2 = Span_{\mathcal{K}} \left\{ dx + dy, dz_1, dw, dz_2 \right\},$$

$$\mathcal{H}_3 = Span_{\mathcal{K}} \left\{ c_3wdx + c_3wdy + (a - d + p_1z_1 + p_2z_2)dz_2, c_3wdc_3 \\ -c_1z_1dz_2, c_3dw + (c_3 - c_2x + c_2y)dz_2 \right\}$$

$\mathcal{H}_4$ and $\mathcal{H}_5$ are not required because the derived flag $\overline{\mathcal{H}}_3$ of $\mathcal{H}_3$ is zero. As a conclusion, the relative degree of any output of the system is less than or equal to 3. To show that $\overline{\mathcal{H}}_3 = 0$, we must verify that

$$dim\overline{\mathcal{H}_3}^{\perp} = 5. \tag{8}$$

The right kernel of $\mathcal{H}_3$ is spanned by

$$g_1 = \begin{pmatrix} 1 \\ -1 \\ 0 \\ 0 \\ 0 \end{pmatrix}, \quad g_2 = \begin{pmatrix} d - a - p_1z_1 - p_2z_2 \\ 0 \\ c_1z_1 \\ (c_2x - c_2y - c_3)w \\ c_3w \end{pmatrix}, \tag{9}$$

the involutive closure $\overline{\{g_1, g_2\}}$ of which has dimension 5:

$$dim\overline{\{g_1, g_2\}} = Rank \begin{bmatrix} \begin{pmatrix} 1 & d - a - p_1z_1 - p_2z_2 & 0 & 0 & 2c_2c_3p_2w \\ -1 & 0 & 0 & 0 & 0 \\ 0 & c_1z_1 & 0 & 0 & 0 \\ 0 & (c_2x - c_2y - c_3)w & -2c_2w & 0 & 0 \\ 0 & c_3w & 0 & 2c_2c_3w & p(x, y, w) \end{pmatrix} \end{bmatrix} = 5.$$

The same results are obtained if we evaluate $dim\overline{\{g, adfg\}}$. That is omitted by the length of the calculations. But, using the software Mathematica we found that $dim\overline{\{g, adfg\}} = 5$ for almost everywhere in $\mathbb{R}_+^5$. The singularities are related to $y = 0$, $z_1 = 0$, and $w = 0$.

As conclusions of this analysis, we have that: (i) the dynamical system ((1)–(5)) is accessible in the space strictly positive of $\mathbb{R}^5$. (ii) However, the system cannot be linearized neither by a static nor a dynamic state feedback since $\mathcal{H}_3$ is not integrable. The maximum dimension of the part that can be linearized is 2. (iii) In comparison with others models in the literature as the 3D-model in [23] (which can be fully linearized by state feedback as it is illustrated in [24]), this model is 'maximally' nonlinear, in the sense that, for any single output, the accessible system can be linearized up to order 2.

Because of the singularities in the analysis of accessibility, we test this property around the equilibria of the system as follows:

The model is not accessible in point A since the vector g and all the ad_f^ig, $i = 1, \cdots$ are 0 for this equilibrium. But it is not surprising because the system cannot leave the free-virus state if there is no infection.

The model is not accessible neither in point B nor in point C since the dimension of $dim\overline{\{g, adfg\}}$ in these points is less than

---

[2] In [4,5] control of the drug dose is exploited so that the inequality is achieved.

5. However, their dimensions are 3 and 4, respectively, then there exist controls which enable to leave the system from the basin of attraction of points B and C.

2.2.3. Model extension including pharmacological concepts

In most of the existing control strategies for the HIV infection dynamics (e.g. [25,26,21]) the control input is hardly applied directly to HIV patients. This is because, instead of the drug dosage, the treatment efficacy is generally considered as the control input. The efficacy varies between 0 (i.e. no medication) and 1 (i.e. full medication) and this is not described in terms of drug amounts. We now discuss the relation between this control input and the drug dosage for the model ((1)–(5)) in consideration of pharmacokinetic and pharmacodynamic models. Note that different HIV models have been used to study the relation between HIV drug concentration and the parameter of viral dynamics in [27,28].

The process of drug administration consists of two phases [7]: the pharmacokinetic phase relating drug dose, intake frequency, and administration route to drug level-time profile in the human body, and the pharmacodynamic phase relating the concentration of the drug at the sites of action to the magnitude of the realised effects.

2.2.3.1. Pharmacokinetic model.
Drugs are mostly prescribed to be taken in a constant dosage at constant time intervals. We assume that drug is absorbed completely and instantaneously, that it distributes in an one-compartmental model of the human body, and that it is eliminated by first order kinetics. The rate of elimination of drug from the human body is modelled by

$$\dot{\sigma} = -k\sigma, \tag{10}$$

where σ is the intracellular amount of drug in the human body at time t and k is the constant first order elimination rate. k is related to the intracellular half-life of the drug $t_{(1/2)}$ by the relation $t_{(1/2)} = \log 2/k$.

The intake of the drug dose is described as an impulsive control input later in this subsection.

2.2.3.2. Pharmacodynamic model.
A number of nonlinear pharmacodynamic models have been studied to fit response–concentration curves empirically [8]. A class of these models is described by the equation

$$\eta(t) = \eta_{max} \frac{C(t)^\gamma}{C(t)^\gamma + 1/Q}, \tag{11}$$

where $\eta(t)$ is the drug efficacy response at plasma concentration of drug $C(t)$, η_{max} is the maximum response, and γ and Q are constants.

As in [8], we set $Q = 1/C_{50}$ where C_{50} is the plasma concentration of drug that reduces the drug efficacy effect by 50% of the maximum response, η_{max}. By [29–31], we can assume that $\gamma = 1$ because the drug FTC-TDF is a combination of two nucleoside reverse transcriptase inhibitors (NRTIs), i.e. emtricitabine and tenofovir.

In the pharmacokinetic model of this paper the human body is modeled as one-compartment. The amount of drug in the body at time t is then obtained by multiplying the plasma concentration $C(t)$ by the so-called 'apparent volume of distribution' V_d and the weight of the human body M. Thus $\sigma(t) = C(t)V_dM$, $\sigma_{50} = C_{50}V_dM$, and

$$\eta(t) = \eta_{max} \frac{\sigma(t)}{\sigma(t) + \sigma_{50}}. \tag{12}$$

For a detailed explanation of the pharmacological consideration see [24].

2.2.3.3. Pharmacological model parameters.
For the pharmacological model (10) and (12) we consider the drug FTC-TDF used in

the experiment of [9], as summarised in Section 2.1. One antiretroviral tablet used in the experiment contains a combination of emtricitabine (FTC 200 mg) and tenofovir (TDF 300 mg): a 500 mg combination known by the brand name Truvada® [32]. To describe the effect of the drug we consider two pharmacological models for FTC and TDF in the system ((1)–(5)). Thus here we study the pharmacological parameters k and σ_{50} for FTC and TDF, namely k_F, k_T, $\sigma_{50,F}$, and $\sigma_{50,T}$ (the subscripts F and T stand for FTC and TDF, respectively).

Although the *in vivo* drug parameters of pharmacokinetics and pharmacodynamics for FTC-TDF are not available yet,[3] the *in vitro* parameters are provided in [34–39]. Note that the pharmacokinetics of FTC and TDF have been evaluated in healthy volunteers and HIV-1 infected individuals and the pharmacokinetics are similar between these two groups [36,37]. The pharmacokinetics of FTC are dose proportional over the dose range of 25–200 mg, not affected by multiple dosing [34,36] while the pharmacokinetics of TDF are independent of dosage over the dose range 75–600 mg following single or repeated administration [35,37].

The authors of [39] have investigated the pharmacokinetics of intracellular FTC and TDF: the geometric mean of FTC intercellular half-life is 39 h with the range of 36–45 h as 90% confidence intervals, while the geometric mean of TDF intercellular half-life is 164 h with the range of 152–190 h as 90% confidence intervals. Thus, for Eq. (10), the first order elimination rate constants for FTC and TDF (i.e. k_F and k_T) are 0.0178/h (0.4266/day) and 0.0042/h (0.1014/day), respectively.

The parameters for volume of distribution for FTC and TDF are 1.4 ± 0.3 l/kg and 0.8 l/kg, respectively [34,35]. The 50% effective concentration value for FTC, known by the brand name Emtriva®, is in the range of 0.0003–0.158 µg/ml (0.0003–0.158 mg/l) [36] and we select its geometric mean 0.0069 mg/l, as in [40]. The 50% effective concentration value for TDF, known by the brand name Viread®, is in the range of 0.04–8.5 µM [37]. The molecular weight of TDF is 635.5 [40], thus the range is 0.025–5.4 mg/l, and we choose the geometric mean 0.3674 mg/l as the 50% effective concentration value for TDF. In addition we assume that the weight of an average person is 70 kg, as in [24,40]. Thus we obtain $\sigma_{50,F}$ as $0.6762 (= 0.0069 \times 1.4 \times 70)$, and $\sigma_{50,T}$ as $20.5744 (= 0.3674 \times 0.8 \times 70)$.

Although we now obtain representative values of the pharmacological parameters, in Section 3.2 we will consider a broad range of the parameters.

2.2.4. Integrated model with impulsive input

The integrated model of ((1)–(5)) with the pharmacological system for FTC and TDF (i.e. (10) and (12)) is given by

$$\dot{x} = \lambda - dx - (1 - \eta_F)(1 - \eta_T)\beta xy, \tag{13}$$

$$\dot{y} = (1 - \eta_F)(1 - \eta_T)\beta xy - ay - p_1 z_1 y - p_2 z_2 y, \tag{14}$$

$$\dot{z}_1 = c_1 z_1 y - b_1 z_1, \tag{15}$$

$$\dot{w} = c_2 xyw - c_2 qyw - b_2 w, \tag{16}$$

$$\dot{z}_2 = c_2 qyw - hz_2, \tag{17}$$

$$\dot{\sigma}_F = -k_F \sigma_F, \tag{18}$$

$$\dot{\sigma}_T = -k_T \sigma_T, \tag{19}$$

---

[3] For control theoretic studies using *in vivo* drug parameters see [24] which are based on the *in vivo* evaluation of [33].

where

$$\eta_F = \eta_{\max,F} \frac{\sigma_F}{\sigma_F + \sigma_{50,F}},$$

$$\eta_T = \eta_{\max,T} \frac{\sigma_T}{\sigma_T + \sigma_{50,T}}.$$

In this model we assume that the antiretroviral effects of both drugs are independent of each other and the subscripts F and T stands for FTC and TDF, respectively. Let $X(t) := [x(t), y(t), z_1(t), w(t), z_2(t), \sigma_F(t), \sigma_T(t)]^T$ and represent model ((13)–(19)) by the equation

$$\dot{X} = F(X). \tag{20}$$

We now consider a conceptual realisation of the experiment of [9] via the model (20). To this end we should introduce impulsive inputs to the system: FTC and TDF intake once daily and possible exposure to HIV during the experiment. These correspond to impulsive changes of the states σ_F, σ_T, and y, respectively. Here we simply assume that the drug intake is impulsive control input of the HIV model as a first approximation, since it is administrated at discrete time instants.

To describe approximately the impulsive inputs we employ a hybrid systems description as in [24], hence the system with impulsive input can be described by

$$\dot{X}(t) = F(X(t)), \quad \text{if} \quad t \notin S_d \cup S_v,$$

$$X^+ = X + V_d, \quad \text{if} \quad t \in S_d,$$

$$X^+ = X + V_v, \quad \text{if} \quad t \in S_v,$$

where V_d is the vector corresponding to the magnitude of change for the states σ_F and σ_T, while V_v is for the state y. S_d is the set of time instants in which the impulsive changes occur for the states σ_F and σ_T, while S_v is for the state y.

To present the impulsive changes of σ_F and σ_T in the hybrid system, we introduce 'oral bioavailability' into V_d, a pharmacokinetic parameter describing the available fraction of an administered drug that reaches the system. Thus

$$V_d = [0, 0, 0, 0, 0, 200 \, (\text{mg}) \times B_F, 300 \, (\text{mg}) \times B_T]^T, \tag{21}$$

where B_F and B_T are the bioavailability of FTC and TDF, respectively. The median of B_F is 0.92 while that of B_T is 0.25 [38]. In addition we assume that once some fraction of the oral dose of FTC-TDF reaches the system, it is fully converted to the activated form intracellularly.

$S_d = \{1, 2, 3, \cdots, T_d\}$, with $T_d = 450$ (day), following the protocol of the experiment in [9]. The values of M_v in $V_v = [0, M_v, 0, 0, 0, 0, 0]^T$ and the set S_v are selected in the next section.

3. Results

In this section we consider that the initial state $X(0)$ is $[10, 0, 10^{-4}, 10^{-4}, 10^{-4}, 0, 0]^T$, which represents the status of a HIV-free patient that corresponds to most of the subjects of the experiment in [9].

We assume $M_v = 10^{-4}$ and $S_v = \{10, 50\}$, which imply that possible contacts with HIV occur at the time instants of the set S_v and a small number of infected cells y emerges by the infusions of the virus into the human body. To follow the experiment protocol we consider that the contact with the virus happens only in the duration of the drug prescription by setting $\max(S_v) < T_d$ and that the drug administration is carried out at $t = 1, 2, 3, \cdots, T_d$.

3.1. Two cases with different pharmacological parameters

In this subsection we simply assume that $\eta_{max,F} = 1$ and $\eta_{max,T} = 1$ based on [29–31] since the drug FTC-TDF is a combination of two NRTIs. This implies that there is not any drug-resistant virus species particularly against FTC and TDF in the system. A different scenario is discussed in the next subsection.

3.1.1. The case with representative pharmacological parameters

Fig. 2 shows the results of the simulation of the experimental protocol in [9] (note the different time scales). We use the proposed hybrid system and the parameter values of k_F, k_T, $\sigma_{50,F}$, and $\sigma_{50,T}$, obtained in Section 2.2.3. In the upper left graph of Fig. 2, the solid line and the dotted line indicate the time histories of σ_F and σ_T, respectively.

The resulting (x, y) trajectory is displayed in Fig. 3. The solid line indicates the (x, y) trajectory. Note that the projection of the initial state is on π_A and that the trajectory is placed within the region $K(x, y) < 0$.

For this simulation the (x, y) point stays extremely close to π_A. Although the level of w is not boosted (since the (x, y) point is located in the region in which $K(x, y)$ is negative for the whole
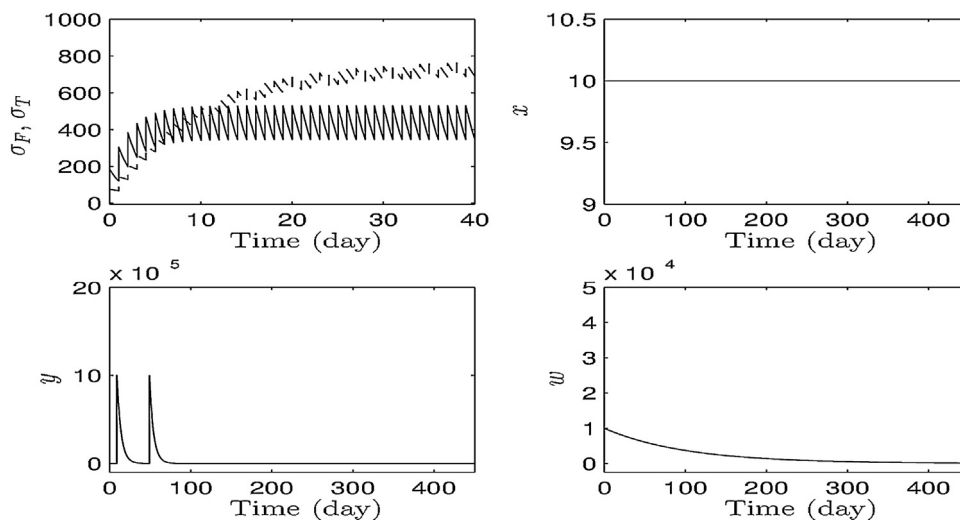

Fig. 2. Results of the numerical realisation of the experiment in [9] via the model (20) with impulsive inputs: $k_F = 0.4266$, $k_T = 0.1014$, $\sigma_{50,F} = 0.6762$, and $\sigma_{50,T} = 20.5744$. In the upper left graph, the solid line and the dotted line indicate the time histories of σ_F and σ_T, respectively. For the implementation of the impulses we set $M_v = 10^{-4}$ and $S_v = \{10, 50\}$. Note the different time scales.
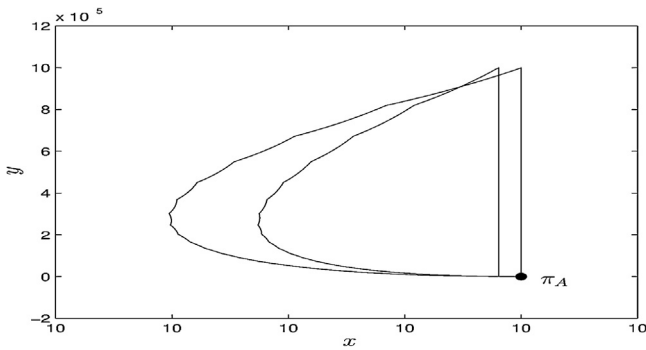
Fig. 3. The (x, y) trajectory resulting from the simulation presented in Fig. 2. The projection of the initial state is on π_A. Note that the trajectory is placed within the region $K(x, y) < 0$.

simulation time), the level of y becomes less than 1.7577×10^{-39} at the end of the simulation. This case might represent the HIV preventive case of [9].

As pointed out in [41,2], our model is deterministic and the virus load (y) cannot be reduced to zero exactly. Note that cell and virus are countable biological object in the human body while the state variables of model (20) are continuous functions of time. Thus we can assume that HIV is eradicated if the virus load is reduced to a sufficiently low level. For example, in [41,2], virus elimination has been studied using a threshold of viral extinction, which could correspond to a virus population less than one cell. We study viral clearance with a threshold of virus load in the next subsection.

3.1.2. The case with comparatively insensitive response to the drug

In Section 2.2.3 we obtain the parameters ($k_F, k_T, \sigma_{50,F}$, and $\sigma_{50,T}$) using representative values such as median or geometric mean, for the pharmacological parameter ranges in [38,36,37,34,35,39]. In this subsection we consider the parameters for a subject showing relatively insensitive response to the HIV drug based on the given ranges of the pharmacological parameters.

In [39] the ranges of intracellular half-life for FTC and TDF are 36–45 and 152–190 h, respectively. With the lower bounds of the ranges the first order elimination rate constants for FTC and TDF are 0.0193/h (0.4621/day) and 0.0046/h (0.1094/day), respectively, as the maximally estimated values for k_F and k_T.

In Section 2.2.3 the 50% effective concentration ranges for FTC and TDF are 0.0003–0.158 mg/l [36] and 0.025–5.4 mg/l [37,40]. The volume of distribution for FTC and TDF are 1.4 ± 0.3 l/kg and 0.8 l/kg, respectively [34,35]. Thus, with the assumption that the weight of an average person is 70 kg, as in [24,40], we obtain that the maximally estimated values of $\sigma_{50,F}$ and $\sigma_{50,T}$ are 18.8020 mg ($= 0.158 \times (1.4 + 0.3) \times 70$) and 302.4 mg ($=5.4 \times 0.8 \times 70$).

Also the ranges of bioavailability of FTC and TDF (B_F and B_T) are 0.831–1.064 and NC^4 –0.45, respectively [38]. In order to present an insensitive subject to FTC-TDF we set $B_F = 0.84$ and $B_T = 0.05$.

Simulation results are presented in Figs. 4 and 5. As in Section 3.1.1, Fig. 4 shows the results of the simulation with the newly estimated values of $k_F, k_T, \sigma_{50,F}, \sigma_{50,T}, B_F$, and B_T (note the different time scales). In the upper left graph of Fig. 4, the solid line and the dotted line indicate the time histories of σ_F and σ_T, respectively.

The resulting (x, y) trajectory is displayed in Fig. 5. The dotted line indicates the set $K(x, y) = 0$ and the solid line indicates the (x, y) trajectory. π_A, π_B, and π_C are the projections onto the $x - y$ plane of Point A, Point B, and Point C, respectively. Note that the projection

---

⁴ NC stands for 'not calculated' [38].

of the initial state is on π_A. The bottom graph is a zoomed-in version of the top graph.

Throughout the simulation the (x, y) point is kept around π_A and π_C with comparatively high and low levels of the states x and y, respectively, consistently with the HIV preventive effect shown in [9]. Furthermore the level of w is boosted over 25, as explained in Section 2.2.2. Given the analysis in Section 2.2.2 the w state is enhanced when the (x, y) point is located in the region in which $K(x, y)$ is positive. If the (x, y) trajectory stays within the region $c_2 xy - c_2 qy - b_2 < 0$ (i.e. the region below the dotted line in Fig. 5), then the concentration of CTL precursor w decreases. Although the (x, y) point stays temporary within the region in which K is negative, the state w is boosted at the end of the simulation.

3.2. Parameter plane of $\eta_{max,F}$ and $\eta_{max,T}$

In the previous subsection we ideally assume that drug-resistant virus does not exist for the two NRTI, FTC and TDF. In this subsection we study a different scenario. Note that anti-retroviral HIV treatment often fails due to the emergence of resistant virus [2].

The emergence of resistant virus results in the reduction of drug effect. Thus, to describe the effect of resistant virus on the drug treatment, we consider variation of the parameters, $\eta_{max,F}$ and $\eta_{max,T}$, which have been assumed equal to one in the previous simulation studies. All other parameters are as in Section 3.1.

To exploit the range of $\eta_{max,F}$ and $\eta_{max,T}$ between 0 and 1, a parameter plane ($\eta_{max,F}, \eta_{max,T}$) is considered. We consider 31 evenly spaced parameter values along each axis of the plane. At every pair of parameter values (i.e. 31×31 pairs) we simulate with impulsive input for 450 days, as in Section 3.1.

After the simulation with impulsive input we determine if the virus load (y) is less than a predefined level of viral extinction threshold, y_{EXT}. If so, then we assume that this case could correspond to the HIV prevention case in the experiment of [9].

This approximate assumption is reasonable in this particular research since in the simulation study we only consider the cases of early stage of HIV infection. For later stages of the infection we cannot assume such approximation because cellular reservoirs, not considered in the model of this paper, would result in HIV persistence even at a very low level of y. For a study similar with this paper on stochastic HIV eradication at early-infection stage, see [42].

If the virus load is not less than the threshold y_{EXT}, then we investigate in which region of attraction, i.e. that of LTNP (Point C) or of AIDS (Point B), the final state of each simulation is located. To this end we additionally simulate for 2000 more days without any input. After this additional input-free simulation we measure the 2-norm distance between this new final state and Point C (or Point B). If the distance to Point C (or Point B) is less than a predefined bound, B_{RA}, then we regard that the state converges to Point C (or Point B). Otherwise we conclude that the state does not converge to Point C or B either.

The investigation results upon the parameter plane are presented in Fig. 6. For the study of this parameter plane, let $y_{EXT} = 10^{-10}$ and $B_{RA} = 0.1$. These results are plotted in the figure with the dot and cross marks, corresponding to convergence to LTNP and AIDS, respectively. The circle marks in the figure represents the case of HIV prevention. Note that if we assume that $\eta_{max,F}$ and $\eta_{max,T}$ are uniformly distributed for HIV infected patients, then we could conclude that HIV infection can be prevented approximately $8.2 (\cong 79/31^2 \times 100)$% by the protocol of the experiment, although the distribution of the two parameters must be investigated in the future works.

As shown in the case of Section 3.1.2, the protocol of the experiment could enhance the immune response against HIV for some subjects. Based on the simulation study beyond the drug administration (e.g. Fig. 6) we could suggest longer follow-up of the subject
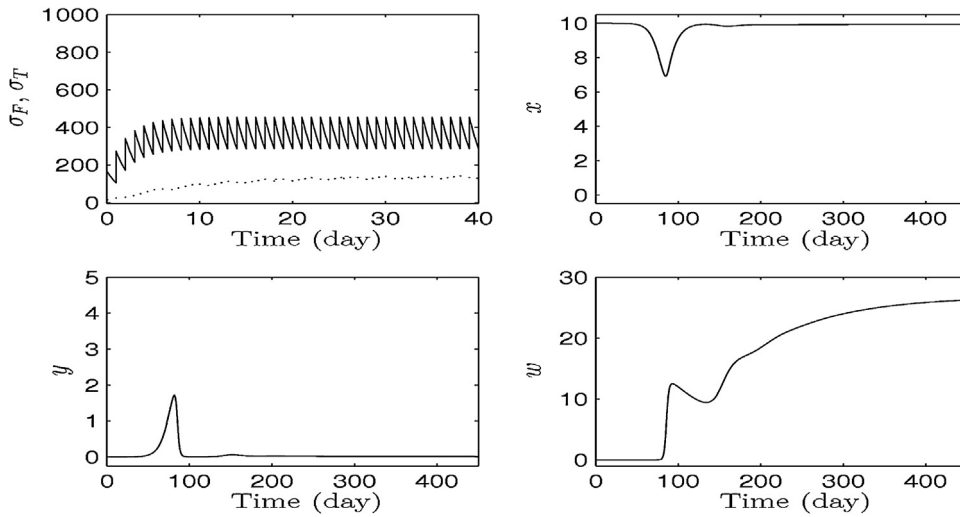
Fig. 4. Results of the numerical realisation of the experiment in [9] via the model (20) with impulsive inputs: $k_F = 0.4621$, $k_T = 0.1094$, $\sigma_{50,F} = 18.8020$, $\sigma_{50,T} = 302.4$, $B_F = 0.84$, and $B_T = 0.05$. These are the estimated values to present a subject showing insensitive drug response, based on the pharmacological parameter ranges in [38,36,37,34,35,39]. In the upper left graph, the solid line and the dotted line indicate the time histories of σ_F and σ_T, respectively. Note the different time scales.
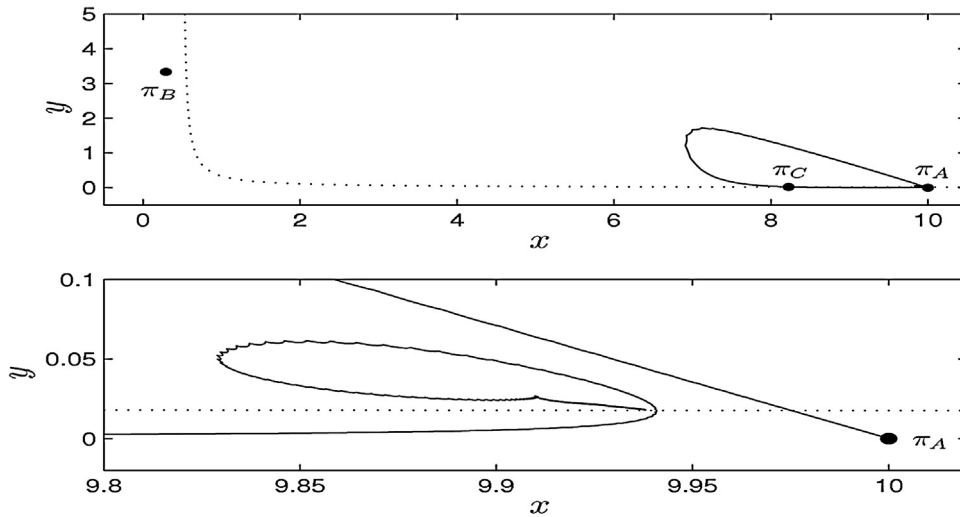
Fig. 5. The (x, y) trajectory resulting from the simulation presented in Fig. 4. The dotted line indicates the set $K(x, y) = 0$ and the solid line indicates the (x, y) trajectory. The projections of Point A, Point B, and Point C is on π_A, π_B, and π_C, respectively.
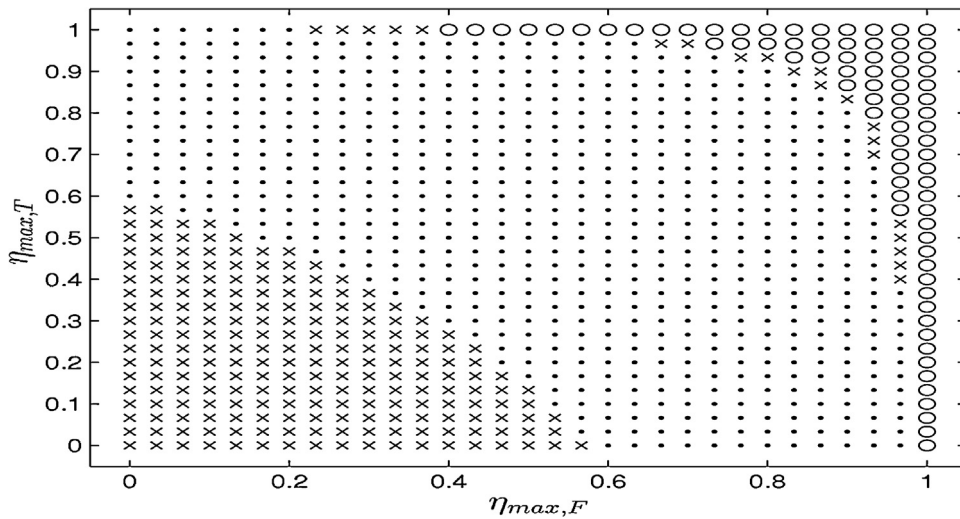

Fig. 6. The convergence results in the parameter plane $(\eta_{max,F}, \eta_{max,T})$. We consider 31 evenly spaced parameter values along each axis. After the simulation with impulsive input, if the virus load is less than viral extinction threshold y_{EXT}, then the corresponding point in the plane is marked with circle. Otherwise we investigate in which of the regions of attraction the final state is located. The dot and cross marks correspond to convergence to LTNP and AIDS, respectively.

of the experiment after cessation of drug therapy in order to determine to which region of attraction the final state of each subject is located.

For the cases of convergence towards AIDS (Point B) we provide two explanations. If the drugs are too ineffective to suppress the virus, then the subject might develop full-blown AIDS (the lower left part of Fig. 6). If the state stays in the region $K(x, y) > 0$ and in the region $y > y_{EXT}$ for the duration of the drug treatment simulation, then the immune system is not boosted and also we cannot conclude that the virus is eradicated (the upper right part of Fig. 6).

4. Discussion

In this paper we have investigated a control scheme for HIV dynamics to enhance the immune response using a model-based approach. The dynamics were analysed. It was shown that this HIV model is accessible but cannot be linearized by a state feedback. This suggests that the model is truly nonlinear. We have proposed the idea of using impulsive input as control mechanism. The control idea has been applied to the HIV model in [3] on the basis of the immune boosting mechanism reported in [5].

To implement the impulsive input we have modified an HIV dynamic model considering the pharmacokinetics and pharmacodynamics of antiretroviral drug and studied numerical realisation of the recently reported clinical experiments in [9]. Through computer simulations of the modified model we have simulated the experiment and analysed the experimental results. By analysing the simulations we have provided some insights into the implications of the experiments. The analysis has shown that the protocol of the experiment might enhance the immune response against HIV.

We can list just a few future works following this paper: Note that the HIV drugs are usually delivered as extended-release formulation [11] although we simply assume that the drug intake is impulsive control input of the HIV model in Section 2.2. Thus further analysis on the modeling of the intestinal absorption of an extended-release oral administration could be one of the future works. In addition, although we simply employ a time-invariant phamacodynamic model (11), we could consider time-varying phamacodynamic model to sophisticate our analysis in the future.

Over the past few years there have been considerable advances in the issues of the suppression of HIV transmission by using antiretroviral drug [17] with new scientific findings including the result in [9]. The new use of Truvada has been approved as a medication to reduce the risk of HIV infection for the first time by the U.S. Food and Drug Administration in July 2012 [43].

Acknowledgments

References

[1] UNAIDS, T.W.H. Organization, AIDS Epidemic Update: 2010, UNAIDS, Geneva, 2010.
[2] M. Nowak, R. May, Virus Dynamics: Mathematical Principles of Immunology and Virology, Oxford University Press, New York, 2000.
[3] D. Wodarz, Helper-dependent vs. helper-independent CTL responses in HIV infection: implications for drug therapy and resistance, J. Theor. Biol. 213 (2001) 447–459.
[4] H. Shim, N. Jo, H. Chang, J. Seo, A system theoretic study on a treatment of AIDS patient by achieving long-term non-progressor, Automatica 45 (2009) 611–622.
[5] H. Chang, A. Astolfi, Activation of immune response in disease dynamics via controlled drug scheduling, IEEE Trans. Autom. Sci. Eng. 6 (2009) 248–255.
[6] H. Chang, C. Moog, A. Astolfi, A control systems approach to HIV prevention with impulsive control input, in: Proc. of Conference on Decision and Control, 2012, pp. 4912–4917.
[7] M. Rowland, T. Tozer, Clinical Pharmacokinetics: Concepts and Applications, Lea & Febiger, Philadelphia, 1980.
[8] M. Gibaldi, D. Perrier, Drugs and the Pharmaceutical Sciences vol. 1: Pharmacokinetics, Marcel Dekker, Inc., New York, 1975.
[9] R.M. Grant, J.R. Lama, P.L. Anderson, V. McMahan, A.Y. Liu, et al., Preexposure chemoprophylaxis for HIV prevention in men who have sex with men, N. Engl. J. Med. 363 (2010) 2587–2599.
[10] C. Cellerai, A. Harari, H. Stauss, S. Yerly, A.-M. Geretti, A. Carroll, et al., Early and prolonged antiretroviral therapy is associated with an HIV-1-specific T-cell profile comparable to that of long-term non-progressors, PLoS ONE 6 (2011) e18164.
[11] M. Battegay, K. Arasteh, A. Plettenberg, J.R. Bogner, J.-M. Livrozet, M.D. Witt, et al., Bioavailability of extended-release nevirapine 400 and 300 mg in HIV-1: a multicenter, open-label study, Clin. Ther. 33 (2011) 1308–1320.
[12] T. Yang, Impulsive control, IEEE Trans. Autom. Control 44 (1999) 1081–1083.
[13] L. Peterson, D. Taylor, R. Roddy, et al., Tenofovir disoproxil fumarate for prevention of HIV infection in women: a phase 2, double-blind, randomized, placebo-controlled trial, PLoS Clin. Trials 2 (2007) e27.
[14] Q. Abdool Karim, S. Abdool Karim, J. Frohlich, et al., Effectiveness and safety of Tenofovir gel, an antiretroviral microbicide, for the prevention of HIV infection in women, Science 326 (2010) 1168–1174.
[15] A. Liu, P. Kittredge, E. Vittinghoff, et al., Limited knowledge and use of HIV post- and pre-exposure prophylaxis among gay and bisexual men, J. Acquir. Immune Defic. Syndr. 47 (2008) 241–247.
[16] M. Mimiaga, P. Case, C. Johnson, S. Safren, K. Mayer, Preexposure antiretroviral prophylaxis attitudes in high-risk Boston area men who report having sex with men: limited knowledge and experience but potential for increased utilization after education, J. Acquir. Immune Defic. Syndr. 50 (2009) 77–83.
[17] The HIV Modelling Consortium Treatment as Prevention Editorial Writing Group, HIV treatment as prevention: models, data, and questions-towards evidence-based decision-making, PLoS Med. 9 (2012) e1001259.
[18] M.S. Cohen, Y.Q. Chen, M. McCauley, T. Gamble, M.C. Hosseinipour, et al., Prevention of HIV-1 infection with early antiretroviral therapy, N. Engl. J. Med. 365 (2011) 493–505.
[19] J.M. Baeten, D. Donnell, P. Ndase, N.R. Mugo, J.D. Campbell, et al., Antiretroviral prophylaxis for HIV prevention in heterosexual men and women, N. Engl. J. Med. 367 (2012) 399–410.
[20] M.C. Thigpen, P.M. Kebaabetswe, L.A. Paxton, D.K. Smith, C.E. Rose, et al., Antiretroviral preexposure prophylaxis for heterosexual HIV transmission in Botswana, N. Engl. J. Med. 367 (2012) 423–434.
[21] R. Zurakowski, A. Teel, A model predictive control based scheduling method for HIV therapy, J. Theor. Biol. 238 (2006) 368–382.
[22] G. Conte, C.H. Moog, A.M. Perdon, Algebraic Methods for Nonlinear Control Systems, 2 ed., Springer, London, 2007.
[23] A. Perelson, P. Nelson, Mathematical analysis of HIV-1 dynamics in vivo, SIAM Rev. 41 (1999) 3–44.
[24] P. Rivadeneira, C. Moog, Impulsive control of single-input nonlinear systems with application to HIV dynamics, Appl. Math. Comput. 218 (2012) 8462–8474.
[25] S. Ge, Z. Tian, T. Lee, Nonlinear control of a dynamic model of HIV-1, IEEE Trans. Biomed. Eng. 52 (2005) 353–361.
[26] B. Adams, H. Banks, H. Kwon, H. Tran, Dynamic multidrug therapies for HIV: optimal and STI control approaches, Math. Biosci. Eng. 1 (2004) 223–241.
[27] Y. Huang, S.L. Rosenkranz, H. Wu, Modeling HIV dynamics and antiviral response with consideration of time-varying drug exposures, adherence and phenotypic sensitivity, Math. Biosci. 184 (2003) 165–186.
[28] Y. Huang, H. Wu, E.P. Acosta, Hierarchical bayesian inference for HIV dynamic differential equation models incorporating multiple treatment factors, Biometr. J. 52 (2010) 470–486.
[29] B.L. Jilek, M. Zarr, M.E. Sampah, S.A. Rabi, C.K. Bullen, J. Lai, L. Shen, R.F. Siliciano, A quantitative basis for antiretroviral therapy for HIV-1 infection, Nat. Med. 18 (2012) 446–451.
[30] L. Shen, S. Peterson, A.R. Sedaghat, M.A. McMahon, M. Callender, et al., Dose–response curve slope sets class-specific limits on inhibitory potential of anti-HIV drugs, Nat. Med. 14 (2008) 762–766.
[31] M.E.S. Sampah, L. Shen, B.L. Jilek, R.F. Siliciano, Dose-response curve slope is a missing dimension in the analysis of HIV-1 drug resistance, Proc. Natl. Acad. Sci. 108 (2011) 7613–7618.
[32] NIAID/NIH, Questions and answers: The iPrEx study: pre-exposure prophylaxis as HIV prevention among men who have sex with men, 2010. [Online], 27 Dec 2011. Available at http://www.niaid.nih.gov/news/QA/Pages/iPrExQA.aspx
[33] M. Legrand, E. Comets, G. Aymard, R. Tubiana, C. Katlama, B. Diquet, An in vivo pharmacokinetic/pharmacodynamic model for antiretroviral combination, HIV Clin. Trials 4 (2003) 170–183.
[34] Emtricitabine PK fact sheet, 2011. [Online], 15 April 2013. Available at http://www.hiv-druginteractions.org/data/FactSheetImages/FactSheet_DrugID_234.pdf
[35] Tenofovir PK fact sheet, 2011. [Online], 15 April 2013. Available at http://www.hiv-druginteractions.org/data/FactSheetImages/FactSheet_DrugID_221.pdf

[36] Gilead Sciences Ltd, Emtriva® Full Prescribing Information, 2011. [Online], 15 April 2013. Available at http://www.gilead.com/pdf/emtriva_pi.pdf

[37] Gilead Sciences Ltd, Viread® Full Prescribing Information, 2011. [Online], 15 April 2013. Available at http://www.gilead.com/pdf/viread_pi.pdf

[38] Gilead Sciences Ltd, Truvada® Full Prescribing Information, 2011. [Online], 15 April 2013. Available at http://www.gilead.com/pdf/truvada_pi.pdf

[39] A. Jackson, G. Moyle, V. Watson, J. Tjia, A. Ammara, et al., Tenofovir, emtricitabine intracellular and plasma, and efavirenz plasma concentration decay following drug intake cessation: implications for HIV treatment and prevention, J. Acquir. Immune Defic. Syndr. (2013), Publish Ahead of Print.

[40] N. Dixit, A. Perelson, Complex patterns of viral load decay under antiretroviral therapy: influence of pharmacokinetics and intracellular delay, J. Theor. Biol. 226 (2004) 95–109.

[41] D. Wodarz, R.M. May, M.A. Nowak, The role of antigen-independent persistence of memory cytotoxic T lymphocytes, Int. Immunol. 12 (2000) 467–477.

[42] S. Khalili, A. Armaou, An extracellular stochastic model of early HIV infection and the formulation of optimal treatment policy, Chem. Eng. Sci. 63 (2008) 4361–4372.

[43] U.S. Food and Drug Administration, FDA approves first medication to reduce HIV risk, in: FDA Consumer Health Information, 2012.